Hydrology and
Earth System
Sciences

Discussions

Open Access

EGU

Water movement through plant roots
Exact solutions of the water flow equation in roots with varying hydraulic properties

Meunier Félicien[1], Couvreur Valentin[2], Draye Xavier[2], Vanderborght Jan[3,4], and Javaux Mathieu[1,3]

[1]Earth and Life Institute-Environment, Université catholique de Louvain, Louvain-la-Neuve, Belgium
[2]Earth and Life Institute-Agronomy, Université catholique de Louvain, Louvain-la-Neuve, Belgium
[3]Forschungszentrum Juelich GmbH, Agrosphere (IBG-3), Juelich, Germany
[4]Division of Soil and Water Management, KU Leuven, Leuven, Belgium

Correspondence to: Félicien Meunier (felicien.meunier@uclouvain.be)

Abstract. In 1978, Landsberg and Fowkes presented a solution of the water flow equation inside a root with uniform hydraulic properties. These properties are root radial conductivity and intrinsic axial conductance, which control, respectively, the radial water flow between the root surface and the axial flow in the xylem. From the solution for the xylem water potential, functions that describe the radial and axial flow along the root axis were derived. In this paper, novel solutions of the water flow equation were developed for roots whose hydraulic properties vary along their axis, which is generally the case for most plants. Six arrangements of radial conductivity and intrinsic axial conductance varying linearly or exponentially with distance from the root tip were analysed. These solutions were subsequently combined to construct root branches with complex hydraulic property profiles. They produced flow distributions different from those in uniform roots. We used the obtained functions for evaluating the impact of root maturation *versus* root growth on water uptake which revealed very contrasted strategies for water uptake. In this study we also looked for optimal root traits that maximize water uptake under a carbon cost constraint. Optimal traits were shown to be highly dependent on the root hydraulic properties. These solutions lead to plant-scale parameters for root water uptake used in ecohydrological models and open consequently new avenues to look for optimal genotype x environment x management interactions.

1 Introduction

Global crop production is negatively affected by drought that is the most significant stress in agriculture (Cattivelli et al., 2008). Drought stress can be defined as the plant's inability to take up and transport the required amount of water to the shoot leading to stomatal closure and reduced yield (Campos et al., 2004). Transferring water from the soil to the shoot, thus preventing leaves from dehydration, is a major role of the root system (McElrone et al., 2013). Root water uptake (RWU) is driven by water potential gradients between soil and atmosphere and is mainly controlled by stomatal regulation, root hydraulic resistance and soil water availability (Volpe et al., 2013). Both root system architecture and hydraulics are key for the location and intensity of water uptake (Leitner et al., 2014). These properties are encapsulated in the concept of root system hydraulic architecture (Lobet et al., 2014). Under high transpiration demand, from the root-soil interface to the evaporative sites, water crosses first radially the root tissues towards the root xylem vessels and flows then up to the leaves (Passioura, 1980).

A continuous solution (i.e., for infinitesimal segments) of water flow equation was developed by Landsberg and Fowkes (1978) for uniform roots. This solution provides continuous water flow functions inside the root branch and highlights the sensitivity of root water uptake on plant hydraulic parameters. To the authors' knowledge, only the uniform root was considered so far for infinitesimal segments.

5   However measurements of root hydraulic properties demonstrated that radial conductivity and intrinsic axial conductance both change with root tissue maturation (Frensch and Steudle, 1989a; Doussan et al., 1998b; Zwieniecki et al., 2002). The anatomical properties of cell layers on water pathways impacts root radial conductivity (Steudle, 2000). The development of endodermal and exodermal apoplastic barriers, first with a Casparian band, then with suberin lamellae and lignified tertiary walls constitutes major hydraulic impedances (Enstone et al., 2002). Aquaporins also play a central role in root radial con-
10   ductivity by facilitating water flow across cell membranes (Chaumont and Tyerman, 2014) and their location and expression change with the maturation of apoplastic barriers (Hachez et al., 2006). Besides, root intrinsic axial conductance increases with abundance, shape and size of xylem vessels, increasing from apical regions with protoxylem to basal regions with late metaxylem vessels (Martre et al., 2000). These maturation steps make younger (distal) root regions more functional for water uptake, while mature (proximal) regions are more adapted to water axial transfer, as confirmed by water flow measurements of
15   Newman (1976) in maize or Zarebanadkouki et al. (2016) in lupine. Uniform root hydraulic properties would on the contrary concentrate water uptake on the proximal region (Meunier et al., Submitted). Figure 1 (top) summarizes estimates and measurements of root radial conductivity and intrinsic axial conductance of primary maize roots as a function of distance to root tip (Frensch and Steudle, 1989b; Frensch et al., 1996; Zwieniecki et al., 2002; Doussan et al., 1998b; Bramley et al., 2007). With an inverse modelling approach coupled to tracer data from Varney and Canny (1993), Doussan et al. (1998b) produced an
20   extensive estimation of root hydraulic property profiles with piecewise functions for both maize primary and lateral roots. The hydraulic conductivity profiles of Zwieniecki comes as well from an inverse modelling exercise (Meunier et al., Submitted). Figure 1 (bottom panels) also illustrates the changes of primary root anatomy with distances to tip as observed by Steudle and Peterson (1998) with cross sections.

     Solving the water flow equation in the root system can be achieved using finite difference (Alm et al., 1992) for any root
25   hydraulic property distribution. Typically the water flow equation in the root system is then solved by segmenting root system hydraulic architecture into small root parts called root segments. Water potentials within the structure are discrete so that each segment has (i) an unique xylem water potential connected to contiguous segment xylem potentials by axial conductances, and (ii) a soil-root interface water potential connected to the segment xylem potential by a radial conductance. Analogically to Ohm's law, radial and axial rates of water flow in each segment are proportional to the associated water potential differences.
30   The water flow equations are solved for the generated root system hydraulic architecture by inverting a conductance matrix of the root system network (Doussan et al., 1998a; Javaux et al., 2008). If root segments were divided into smaller sub-segments though, water potentials and flows would slightly vary in each segment. The result is consequently an approximation of the exact solution that would be obtained for root segments of infinitesimal length, but of course in such case numerically inverting a conductance matrix of infinite size would be impossible because of computational requirements.
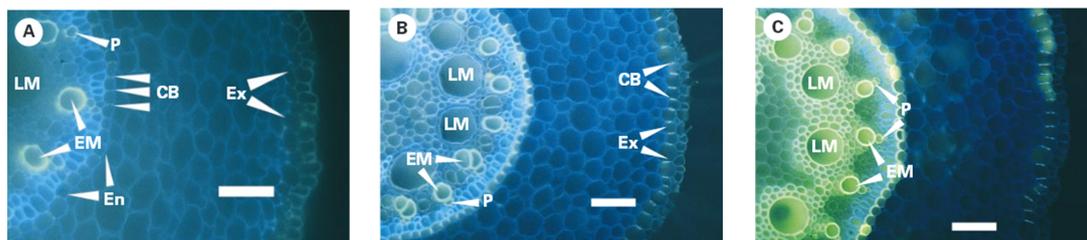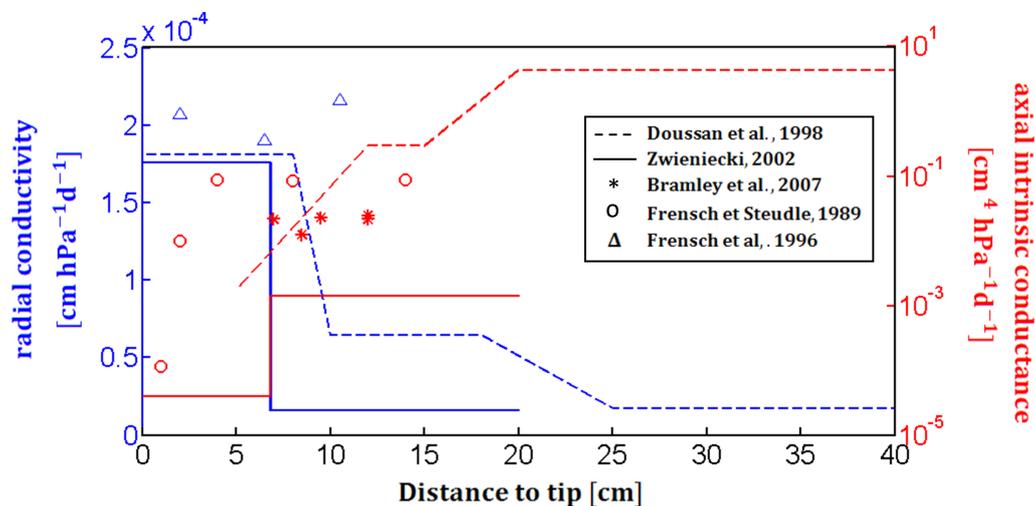
Figure 1. Top: Maize radial conductivity (left axis) and intrinsic axial conductance (right axis) of primary roots as measured in several studies. Bottom: maize primary root cross-sections obtained at different development stages. The root cross-sections are the work of Steudle and Peterson (1998). The scale bars are 100 microns long. Ex = exodermis, En = endodermis, CB = casparian band, P = protoxylem, EM = early metaxylem, LM = late metaxylem. (a) Immature Ex, En with CB, mature P, mature EM and immature LM, (b) mature Ex, En with asymmetrically thickened walls, mature P and EM, immature LM (c) similar to (b) with mature LM. Reproduced by courtesy of Steudle and Peterson.

In this paper we show that uniform root property assumption may be relaxed and yet analytical solutions of the water flow equation in roots are within our reach. Our objective is to present novel mathematical solutions of the water flow equation in roots with non-uniform radial and axial hydraulic properties. This widens the solution of Landsberg and Fowkes (1978) to roots growing at rates potentially decoupled from tissue maturation rate and opens new avenues for looking for root system ideotypes, i.e. root systems perfectly adapted to their environment.

In the following, we only consider root branches without laterals. Consequently we sometimes use simply the word roots for root branches. When used, the terms root stretch or root segment designate a portion of the root branch characterized by specific root properties. The solutions we developed here will be used as building blocks for branched root systems in further studies.

2 Theory

2.1 Water flow equation in a root branch

Assuming that root branch water content does not fluctuate, water mass balance in infinitesimal root segments of a cylindrical branch of radius $r\,[\mathrm{L}]$ and total length $l\,[\mathrm{L}]$ under uniform soil-root interface water potential yields (Landsberg and Fowkes, 1978):

$$\frac{dJ_x(z)}{dz} = -2\pi r k_r(z)\left(\Psi_x(z) - \Psi_{soil}\right) \tag{1}$$

where $J_x\,[\mathrm{L^3 T^{-1}}]$ is the axial flow of water inside the root, $k_r\,[\mathrm{L T^{-1} P^{-1}}]$ is the root radial conductivity, $\Psi_x\,[\mathrm{P}]$ is the xylem water potential and $\Psi_{soil}\,[\mathrm{P}]$ is the uniform water potential at soil-root interface, and $z\,[\mathrm{L}]$ is the distance from the root tip along the root axis. The axis z is always chosen parallel to the root axis. Note that the right-hand side term corresponds to root radial flow rate per unit root length $q_r\,[\mathrm{L^2 T^{-1}}]$:

$$q_r = -2\pi r k_r(z)\left(\Psi_x(z) - \Psi_{soil}\right) \tag{2}$$

Axial flow is driven by the water potential gradient in the xylem vessels:

$$J_x(z) = -k_x(z)\frac{d\Psi_x(z)}{dz} \tag{3}$$

with $k_x\,[\mathrm{L^4 T^{-1} P^{-1}}]$ the intrinsic axial conductance of the root. Combining Eq. (1) and (3), we obtain:

$$\frac{d}{dz}\left(k_x(z)\frac{d\Psi_x(z)}{dz}\right) = 2\pi r k_r(z)\left(\Psi_x(z) - \Psi_{soil}\right) \tag{4}$$

which is the general equation of water flow equation in roots.

2.2 General solutions of root water flow

The differential Eq. (4) can be solved for various kinds of root properties and boundary conditions. Since Eq. (4) is a second-order differential equation, its general solution is:

$$\Psi_x(z) = \Psi_{soil} + c_{1,i}f_{1,i}(z) + c_{2,i}f_{2,i}(z) \tag{5}$$

Where $c_{1,i}$ and $c_{2,i}$ are constants whose values depend on root hydraulic properties and boundary conditions and $f_{1,i}$ and $f_{2,i}$ are differentiable functions of z whose type depends on the root hydraulic property profiles. The subscript i as it will be further explained is used to distinguish root stretches. It can vary between 1 and N, the total number of stretches.

Hydrology and
Earth System
Sciences

Discussions

For simple functions $k_x(z)$ and $k_r(z)$ (i.e. uniform, linear and exponential), we derive analytical expressions for $f_1(z)$ and $f_2(z)$, $c_{1,i}$ and c_22,i in Appendix A. However, $k_x(z)$ and $k_r(z)$ profiles generally correspond to piecewise collections of these simple functions. Hence, we establish a procedure to compute analytical expressions of water flow in root stretches connected in series with contrasted hydraulic property profiles. Figure 2 presents a sketch of a root branch made of five stretches delimited by dashed vertical lines.

Deriving the coefficients $c_{1,i}$ and $c_{2,i}$ in any root stretch i requires boundary conditions at the limits of each stretch (i.e., at $z = l_{i-1}$, the root stretch i's distal end and at $z = l_i$, its proximal end). The bottom flux boundary condition at the distal end of stretch i is called J_{i-1} $[\mathrm{L}^3\mathrm{T}^{-1}]$, and the xylem water potential at the proximal end of stretch i is $\Psi_{proximal,i}$ $[\mathrm{P}]$ as it appears in Fig. 2:

$$
\begin{cases}
J_x(l_{i-1}) = J_{i-1} \\
\Psi_x(l_i) = \Psi_{proximal,i}
\end{cases}
\tag{6}
$$

Note that $J_0 = 0$ (no axial flow at the root tip), and $\Psi_{proximal,N} = \Psi_{collar}$ (the xylem water potential at the proximal end of the last root stretch N is that of plant collar).
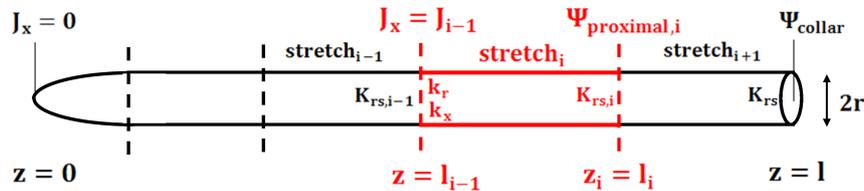
Figure 2. Root branch made of five stretches (the dashed vertical lines are stretch boundaries). For root stretch i, boundary condition at $z = l_{i-1}$ (distal end) is the water flow J_{i-1} and at $z = l_i$ (proximal end) the xylem water potential $\Psi_{proximal,i}$. For details, see text.

2.3 Macroscopic root hydraulic properties

At this point, as only J_0 and $\Psi_{proximal,N}$ are predefined full root boundary conditions, none of the root stretches has both boundary conditions known (J_{i-1} and $\Psi_{proximal,i}$) so the water flow solution is not straightforward unless the root branch is made of a single stretch. To solve this problem, the concept of root macroscopic parameters is used.

The root macroscopic parameters consist in the root system conductance K_{rs} $[\mathrm{L}^3\mathrm{T}^{-1}\mathrm{P}^{-1}]$ and the Standard Uptake Density SUD $[\mathrm{L}^{-1}]$ (Meunier et al., Submitted). These parameters are used in soil-root water transfer models that stem from principles of water flow in root hydraulic architecture but do not rely on the associated geometrical description of root system (Couvreur

et al., 2012). Hence the transpiration stream is directly collected from the soil, for instance as sink terms at each soil location (Couvreur et al., 2014). They are calculated in homogeneous soil conditions and are defined as:

$$
\begin{cases}
K_{rs,i} = \frac{J_x(l_i)}{\Psi_{soil} - \Psi_x(l_i)} \\
SUD_i(z) = \frac{q_r(z)}{J_x(l_i)}
\end{cases}
\tag{7}
$$

It is worth noting that the macroscopic parameters are always independent of the boundary conditions: they only include the root geometric (radius and length) and hydraulic properties ($k_r(z)$ and $k_x(z)$). The macroscopic parameters are calculated by a recursive equation:

$$
\begin{cases}
K_{rs,i} = k_x(l_i) \frac{\left(-K_{rs,i-1}f_{2,i}(l_{i-1}) + f'_{2,i}(l_{i-1})k_x(l_{i-1})\right)f'_{1,i}(l_i) + \left(K_{rs,i-1}f_{1,i}(l_{i-1}) - f'_{1,i}(l_{i-1})k_x(l_{i-1})\right)f'_{2,i}(l_i)}{K_{rs,i-1}f_{1,i}(l_{i-1})f_{2,i}(l_i) - K_{rs,i-1}f_{1,i}(l_i)f_{2,i}(l_{i-1}) - f'_{1,i}(l_{i-1})f_{2,i}(l_i)k_x(l_{i-1}) + f_{1,i}(l_i)f'_{2,i}(l_{i-1})k_x(l_{i-1})} \\
SUD_i(z) = \frac{2\pi r k_r(z)}{k_x(l_i)} \frac{\left(-K_{rs,i-1}f_{2,i}(l_{i-1}) + f'_{2,i}(l_{i-1})k_x(l_{i-1})\right)f_{1,i}(z) + \left(K_{rs,i-1}f_{1,i}(l_{i-1}) - f'_{1,i}(l_{i-1})k_x(l_{i-1})\right)f_{2,i}(z)}{\left(-K_{rs,i-1}f_{2,i}(l_{i-1}) + f'_{2,i}(l_{i-1})k_x(l_{i-1})\right)f'_{1,i}(l_i) + \left(K_{rs,i-1}f_{1,i}(l_{i-1}) - f'_{1,i}(l_{i-1})k_x(l_{i-1})\right)f'_{2,i}(l_i)}
\end{cases}
\tag{8}
$$

as demonstrated in Appendix B. Let us note that the $K_{rs,i}$ and SUD_i as they have been defined in Eq. (7) represent the root branch macroscopic parameters after addition of i stretches ignoring thus the root stretches after the considered zone. However they are useful to solve the water flow equation when dealing with multiple-stretched root branches. Indeed in such a start, we start with the calculation of $K_{rs,1}$ (i.e., the conductance of the most distal stretch) using Eq. (8) (with $K_{rs,0} = 0$ because the very distal axial flow is null). The obtained $K_{rs,1}$ is then used as $K_{rs,i-1}$ to calculate the effective conductance of the distal part from the second stretch $K_{rs,2}$ using Eq. (8). This procedure is then used again to derive the $K_{rs,i}$ of all stretches until the root collar is reached. The obtained set of $K_{rs,i}$'s or $K_{rs,i-1}$'s are then used to calculate the coefficients $c_{1,i}$ and $c_{2,i}$ for the different stretches using (demonstration given in Appendix B):

$$
\begin{cases}
c_{1,i} = \frac{(\Psi_{proximal,i} - \Psi_{soil})\left(-K_{rs,i-1}f_{2,i}(l_{i-1}) + f'_{2,i}(l_{i-1})k_x(l_{i-1})\right)}{K_{rs,i-1}f_{1,i}(l_{i-1})f_{2,i}(l_i) - K_{rs,i-1}f_{1,i}(l_i)f_{2,i}(l_{i-1}) - f'_{1,i}(l_{i-1})f_{2,i}(l_i)k_x(l_{i-1}) + f_{1,i}(l_i)f'_{2,i}(l_{i-1})k_x(l_{i-1})} \\
c_{2,i} = \frac{(\Psi_{proximal,i-1} - \Psi_{soil})\left(K_{rs,i-1}f_{1,i}(l_{i-1}) - f'_{1,i}(l_{i-1})k_x(l_{i-1})\right)}{K_{rs,i-1}f_{1,i}(l_{i-1})f_{2,i}(l_i) - K_{rs,i-1}f_{1,i}(l_i)f_{2,i}(l_{i-1}) - f'_{1,i}(l_{i-1})f_{2,i}(l_i)k_x(l_{i-1}) + f_{1,i}(l_i)f'_{2,i}(l_{i-1})k_x(l_{i-1})}
\end{cases}
\tag{9}
$$

Since in Eq. (9), only the pressure head at the proximal part of the stretch is needed as a boundary (in addition to the distal root conductance), the calculation is started at the proximal part of the root system where the root collar potential Ψ_{collar} is known. The obtained $c_{1,i}$ and $c_{2,i}$ for the proximal stretch are subsequently used in Eq. (5) to calculate the water potential at the distal part of the stretch. The water potential is then used to calculate the coefficients of the next stretch (towards the root tip). This procedure is used until the most distal stretch is reached. As SUD depends on the collar water flow, it can not be calculated for each zone. However it can be derived at the end on the procedure when the xylem water potential is defined

everywhere inside the root and when the total root conductance has been already calculated. Note that we use the terms K_{rs} and SUD for $K_{rs,N}$ and SUD_N which corresponds to the macroscopic parameters of the entire root branch:

$$
\begin{cases}
K_{rs} = \frac{J_x(l)}{\Psi_{soil} - \Psi_x(l)} \\
SUD(z) = \frac{q_r(z)}{J_x(l)}
\end{cases}
\tag{10}
$$

2.4 Resolution of the root water flow equation

5   We here analyse six cases: the uniform root (already developed by Landsberg and Fowkes (1978)), a root branch with linear root hydraulic property profiles and a root branch with exponential root hydraulic property profiles. For the two latter cases, the radial conductivity and the intrinsic conductance may change alone or simultaneously. Table 1 summarizes the six cases with the corresponding local hydraulic properties.

The parameters used in Table 1 are gathered as well as their units in Table 2 (two first columns). To simplify the solutions
10   of the root water flow equation, some parameters are combined. The expression of the adjusted parameters is also contained in Table 2 with their corresponding units (two last columns).

Table 3 summarizes the solutions of the root water flow equation obtained for the six considered cases. The resolution details are provided in Appendix A.

These functions can be combined in complex root with several root stretches using the flux boundary conditions (9) as
15   explained in the previous section.

Figure 3 shows the procedure to solve the water flow problem in a root with variable hydraulic properties. First we need to know whether the root is made of one or several stretches. Then we have to determine the coefficients $c_{1,i}$ and $c_{2,i}$ for each single zone, $i \in [1\ N]$ by determining the type of root stretch we deal with and by using Eq. (9). Thanks to these coefficients, we obtain the root conductance after addition of each stretch by applying Eq. (8). Finally we calculate the xylem potential, the
20   axial flow, the radial flow per root branch length and the macroscopic parameters using the appropriate equations and analytical functions given in Table 3. The corresponding equations are mentioned in the figure.

If the root branch is made of only one stretch, there is no need to calculate intermediary root conductances. The solutions of Table 3 are then used with the no flux boundary condition coefficients to obtain the macroscopic parameters as well as the water xylem potentialn radial and axial water flow profiles along the root axis. This particular case is analysed in Appendix C.
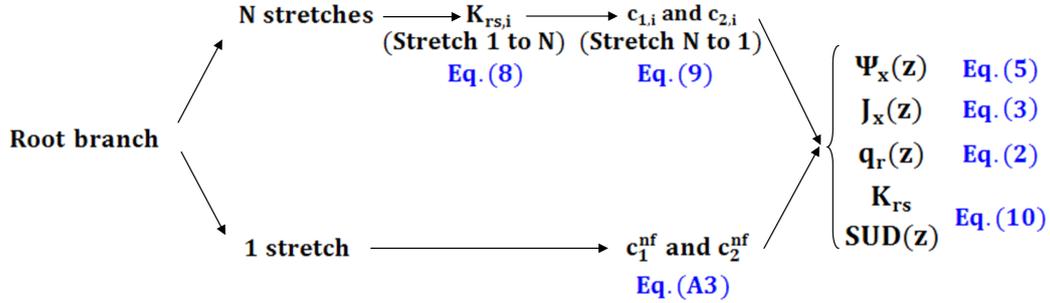
Figure 3. Flowchart of the water flow equation resolution in roots with heterogeneous hydraulic properties

2.5 Properties of a growing root

In this section we introduce the time dimension. As in many studies, the properties are measured as a function of emerging time instead of distance to tip, we provide here a tool to switch from one to another. Basically an equation of the root elongation rate is required. We consider here an instantaneous growth rate $v(t) \, \mathrm{LT^{-1}}]$, function of the actual time $t \, [\mathrm{T}]$, given by:

$$v(t) = v_0 exp\left(\frac{-v_0}{l_{max}}t\right) \tag{11}$$

where $v_0 \, [\mathrm{LT^{-1}}]$ is the initial elongation rate and $l_{max} \, [\mathrm{L}]$ is the root maximal length (Pagès et al., 2004). When the transition ages, $age_i \, [\mathrm{T}]$, are known, the stretch lengths, $stretch_i(t) \, [\mathrm{L}]$ are given by:

$$stretch_i(t) = \begin{cases} 0, t < age_i \\ l_{max}\left(1 - exp\left(\frac{-v_0}{l_{max}}(t - age_i)\right)\right), t \geq age_i \text{ and } t \leq age_{i+1} \\ l_{max}\left(exp\left(-\frac{v_0}{l_{max}}(t - age_{i+1})\right) - exp\left(-\frac{v_0}{l_{max}}(t - age_i)\right)\right), t > age_{i+1} \end{cases} \tag{12}$$

See Appendix D for details.

3 Model Testing

3.1 Model Illustration

We now illustrate some of the results developed in Sect. 2 and related applications. Figure 4 represents how the radial conductivity (a) and the intrinsic axial conductance (b) depend on distance to tip for three different roots. The blue solid lines represent a root with uniform hydraulic properties while the dashed and dotted are roots with linear and exponential hydraulic property profiles (radially and axially), respectively. The numerical values are chosen so that the collar axial flows $J_x(l)$ of the three

Hydrology and
Earth System
Sciences

Open Access

Discussions

roots are the same under identical potential difference between the soil-root interface and the root collar. Their conductance K_{rs} is thus equal.
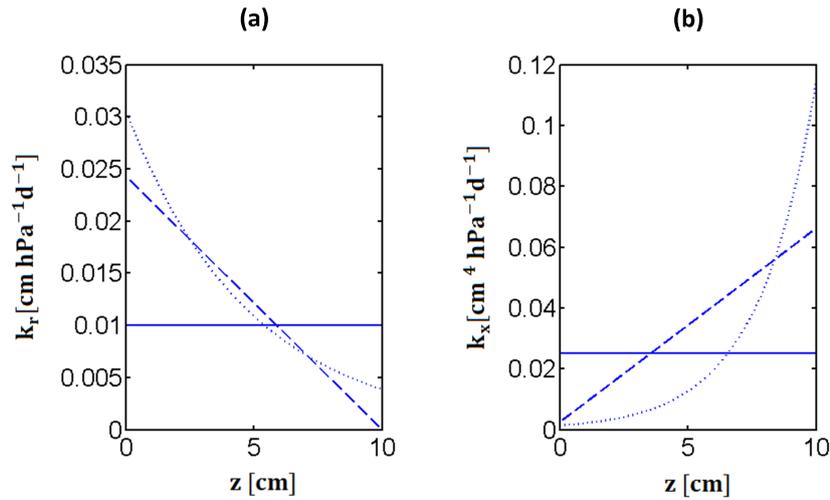
Figure 4. Local radial conductivity (a) and intrinsic axial conductance (b) of a root branch with uniform hydraulic properties (solid blue line), a root branch with linear hydraulic profiles (dashed lines) and a root branch with exponential hydraulic profiles (dotted lines). The origin of the z-axis is at the root tip.

Solutions of the water flow equation are shown in Fig. 5 for the three roots (the legend is the same as in the previous figure). In subplot (a) xylem water potential obtained thanks to Eq. (A1) (solid line), (A4) (dashed lines) and (A5) (dashed-dotted line)

5   are represented when considering a constant Ψ_{collar} of -3000 hPa and a uniform soil water potential of 0 hPa. In subplot (b) and (c) the radial flow per root branch length q_r and the axial water flow J_x are obtained applying respectively Eq. (2) and Eq. (3) to the different cases.

Even if the collar axial flow is identical for each root, the xylem water potential and the root water uptake profiles look totally different. The drop in potential is more homogeneously distributed along the roots with heterogeneous properties. While q_r is

10   a monotonic, increasing function in the case of the uniform root, its maximal value is not reach at the root collar in the two other situations: the maximal uptake is not located at the root collar. Consequently the axial flow first increases faster for the roots with non-uniform properties before slowing down to reach the same value at the root collars.

We define two root parameters combining root hydraulic and geometric properties:

$$\begin{cases} \tau(z) = \sqrt{\dfrac{2\pi r k_r(z)}{k_x(z)}} \\ \kappa(z) = \sqrt{2\pi r k_r(z) k_x(z)} \end{cases}$$

15   The units of these root parameters are $[\mathrm{L}^{-1}]$ and $[\mathrm{L}^{-3}\mathrm{P}^{-1}\mathrm{T}^{-1}]$, respectively. These parameters have the same definitions than in the case of the uniform root but they depend now on the position along the root axis (see Appendix A.1). τ and κ are
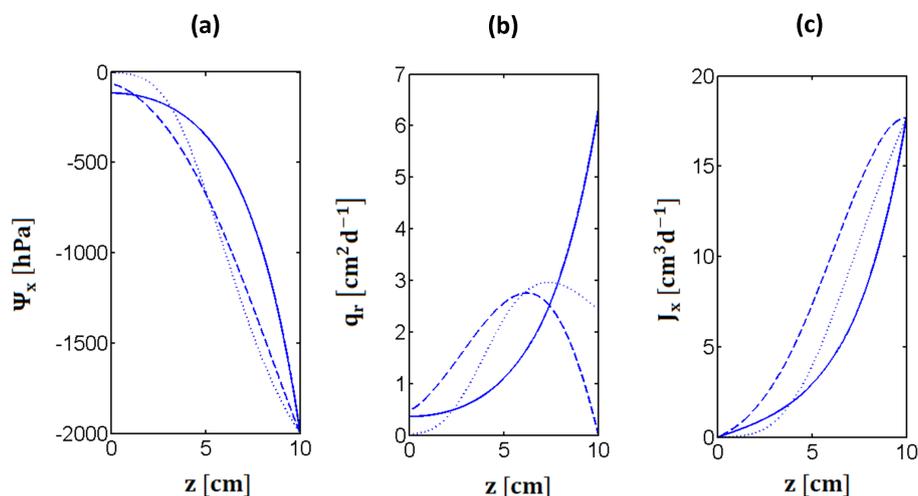
Figure 5. Solutions of the root water flow equation: xylem water potential (a), radial water flow per root branch length (b) and axial water flow (c) of a root with uniform properties (solid blue line), a root with linear hydraulic profiles (dashed lines) and a root with exponential hydraulic profiles (dotted lines). The origin of the z-axis is at the root tip.

represented in Fig. 6, subplots (a) and (b), respectively. These parameters are constant for the uniform root. τ is monotonically decreasing for the non-uniform roots because the intrinsic axial conductance is decreasing and the radial conductivity is increasing along the root axis. The root with linear hydraulic profiles has a non-monotonic κ while this parameter is always increasing for the root with exponentially changing hydraulic properties. These hydraulic parameters must be set in relation with the root macroscopic parameters represented in the bottom line of Fig. 6. In subplot (a) SUD is represented along the

5 z-axis (note that this subplot is the same as the second subplot of Fig. 5 except that the curve is now normalized so that its integral on total root branch length is one). K_{rs} is plotted as a function of the root length in subplot (b). As in the uniform root case τ indicates how fast the root system conductance changes and how homogeneous the water uptake along the root axis under homogeneous soil conditions is. κ is an indicator of the maximal possible root system conductance. It is worth noting

10 that the root system conductances differ very much between the cases. Depending on how k_r and k_x vary along the root, K_{rs} might even decrease with increasing root length (linear root case). This occurs when additional segments with a low k_r are added so that the extra inflow across these segments does not compensate for the extra pressure head loss due to axial flow through these segments. However, if the k_r decrease with root length levels off and the k_x increases stronger with increasing root length, as it is the case in the exponential scenario, the root system conductance may increase steadily with root length.

15 **3.2   Comparison between uniform and heterogeneous root hydraulic profiles**

Here we compare root branches with complex hydraulic profiles (as they have been observed) and uniform root hydraulic properties in terms of distribution of water xylem potential, radial and axial flows and macroscopic parameters. We therefore
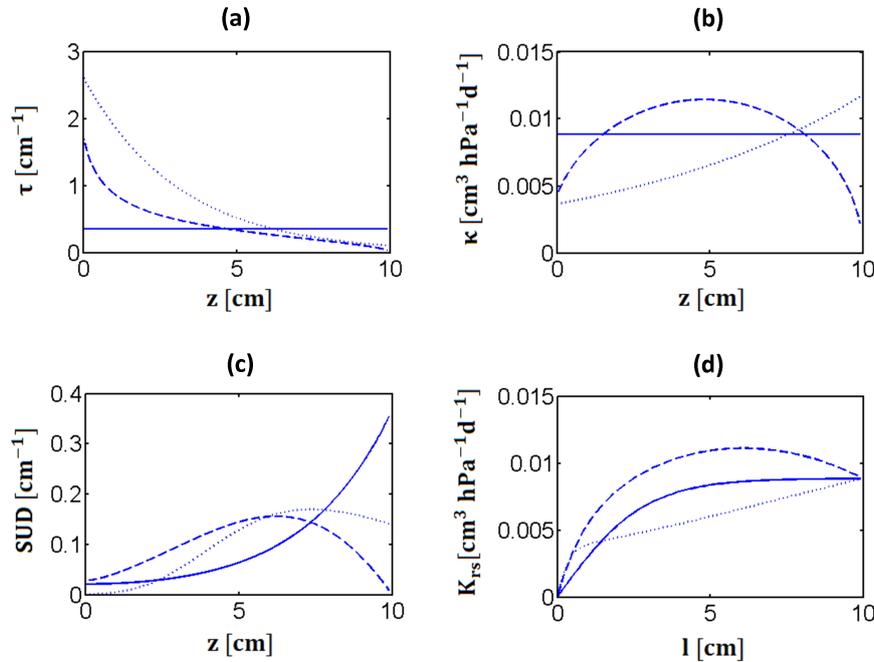
Figure 6. Local (top line) and macroscopic (bottom line) hydraulic parameters: τ (a), κ (b), SUD (c) and K_{rs} (d) of a root branch with uniform properties (solid blue line), a root branch with linear hydraulic profiles (dashed lines) and a root branch with exponential hydraulic profiles (dotted lines).

investigate whether uniform root hydraulic properties could mimic more complex situations. Two cases are examined: the lateral lupine roots studied by Zarebanadkouki et al. (2016) and the lateral maize roots analysed by Doussan et al. (1998b).

3.2.1 A lupine lateral root: example of a single stretch root branch

First we analysed the water uptake in lupine lateral root described by Zarebanadkouki et al. (2016) as an illustration of the
5 single-stretch root model solution. These authors observed water uptake along lateral root compatible with exponential changes in radial conductivity and intrinsic axial conductance along root axis. In Fig. 7 the hydraulic properties (subplots (a) and (b) for the radial conductivity and the intrinsic axial conductance, respectively), together with the pressure head (c) and radial flow (d) distribution along the root axis are given by the blue solid lines. These results are compared with three alternative models, where the root axis has uniform hydraulic properties with minimal (red dashed line, subplots (a) and (b)), maximal (red dotted
10 line, subplots (a) and (b)) and mean (red dashed-dotted line, subplots (a) and (b)) values in order to verify whether uniform properties could reproduce the uptake distribution properly. The third and fourth subplots in Fig. 7 show the main solutions of the root water flow equation: xylem water potential and axial water flow, respectively. The complex root branch can not be properly represented by uniform root properties. The water potential drop of the complex root is again more uniformly

Hydrology and
Earth System
Sciences
Discussions

Open Access

distributed along the root axis in the case of heterogeneous properties because the radial conductivity is maximal at the root tip and the intrinsic axial conductance increases progressively.
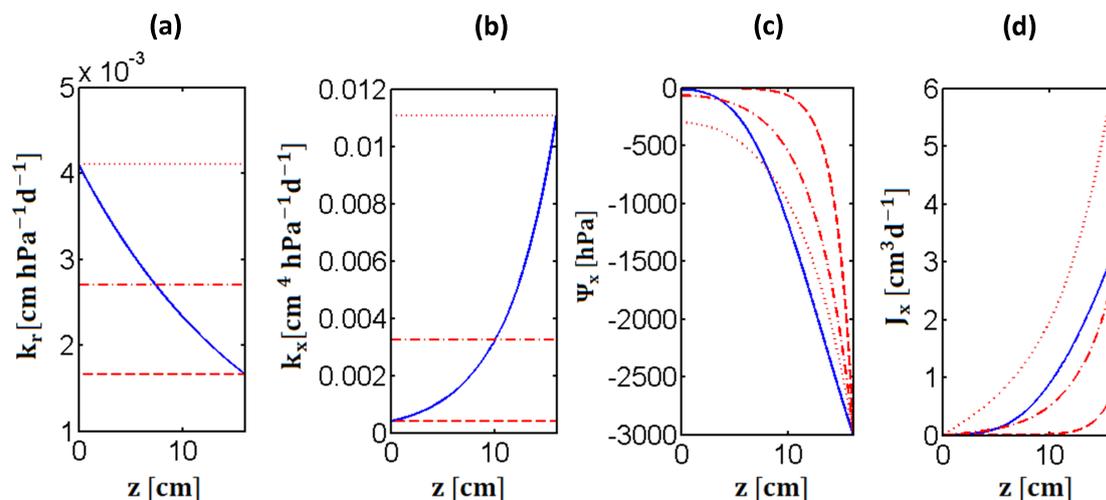
Figure 7. Distributions of radial conductivity (a), intrinsic axial conductance (b), xylem water potential (c) and axial water flow (d) for a lupine lateral root. We used local hydraulic properties obtained by Zarebanadkouki et al. (2016) (blue solid line) or equivalent properties (red lines) with minimal (dashed), maximal (dotted) and mean (dashed-dotted) values. The origin of the z-axis is at the root tip.

We can estimate the macroscopic parameters for these lateral lupine roots (SUD and K_{rs}) as a function of the root branch length with our solutions for the water flow equations. The distribution of these two parameters is shown in Fig. 8 for different hypotheses: heterogeneous root properties as obtained by Zarebanadkouki et al. (2016) or uniform mean (dashed-dotted red line), minimal (dashed red line) and maximum (dotted red line) hydraulic properties. We observe that these macroscopic parameters are poorly represented by the uniform root branches. A complex root branch can not be accurately approximated by an equivalent root branch with uniform hydraulic properties because it generates complex macroscopic parameter functions.

3.2.2 A maize lateral root: example of a root branch with multiple stretches

Similarly we examine the case of a lateral maize root as described by Doussan et al. (1998b). This constitutes an illustration of the multiple-stretches root branch. In their study, they described intrinsic axial conductance and radial conductivity as stepwise functions of the root age or distance to tip. They justified it by the root tissue maturation and development. These functions are shown in the two first subplots of Fig. 9: the radial conductivity (a) and the intrinsic axial conductance (b) as obtained by the authors are presented with blue solid lines. These subplots are equivalent to the Fig. 4B of the study of Doussan et al. (1998b) when a constant elongation rate of 1 cm per day is assumed. We removed the isolated distal region (whose intrinsic axial conductance is null and that consequently does not influence the rest of the root). The red dashed, dotted and dashed-dotted lines correspond to roots with uniform properties with minimal, maximal and mean values observed for both hydraulic properties, respectively. The solution of the water flow equation is represented for the four cases in Fig. 9, subplots (c) and (d).
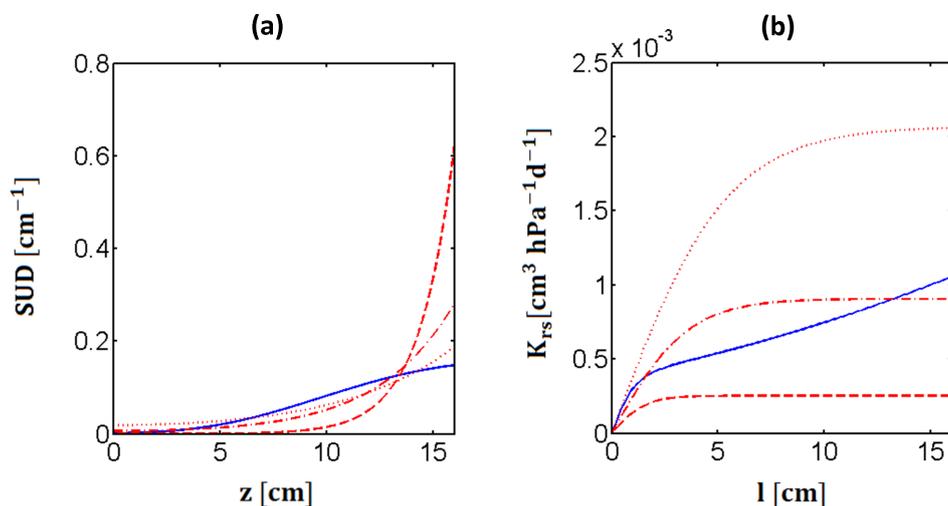
Figure 8. Macroscopic parameters: final SUD (a) and K_{rs} changes (b) for a growing lateral root branch of lupine with the local hydraulic properties measured by Zarebanadkouki et al. (2016) (blue solid line) or the equivalent uniform root branches (red lines) with minimal (dashed), maximal (dotted) or mean (dashed-dotted) hydraulic property values.

When we compare the Doussan distribution of water radial flow per root branch length and potential with those of uniform hydraulic property models, we observe that it is not possible to represent its complex behaviour with an apparent/effective uniform model. The drop of water potential is much steeper with heterogeneous than with homogeneous properties (red lines). The decrease in water potential and the increase in axial flow are far more uniform along the composite root than along the homogeneous roots. This is in fact similar to what we found for the case of the single stretch root branch with changing root properties.

We used Eq. (8) to derive the macroscopic parameters of the four root branches (the complex root branch and the three uniform root branches). Again both the SUD and the K_{rs} could not be well represented by uniform roots. It is indeed impossible with these solutions to represent non-monotonic functions as the standard uptake density (subplot (a), Fig. 10) and the root conductance (subplot (b), Fig. 10).
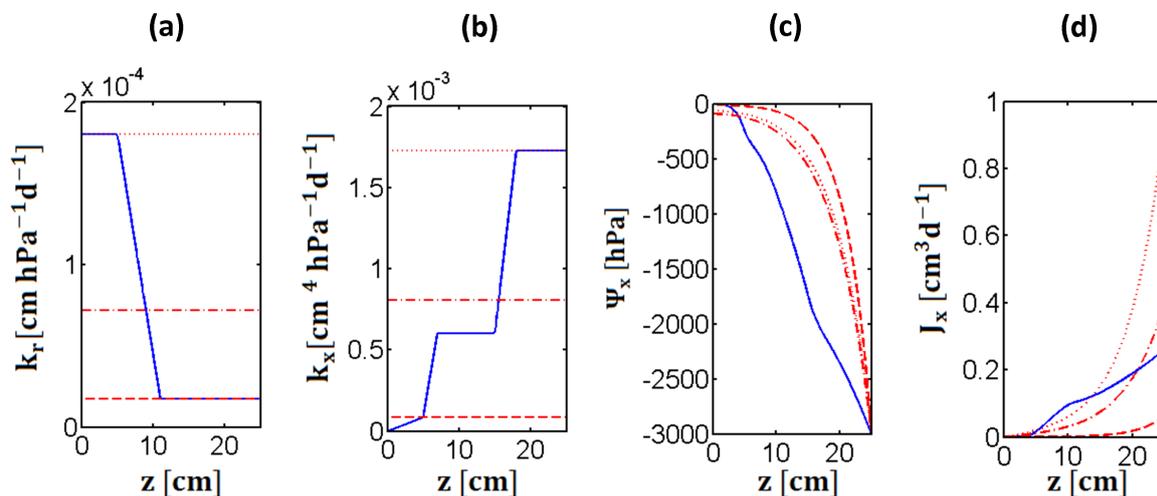
Figure 9. Distributions of radial conductivity (a), intrinsic axial conductance (b), xylem water potential (c) and axial water flow (d) in a maize lateral root branch. We used hydraulic properties obtained by Doussan et al. (1998b) (blue solid line) for a maize lateral root branch or equivalent properties (red lines) with minimal (dashed), maximal (dotted) or mean (dashed-dotted) values. The origin of the z-axis is at the root tip.
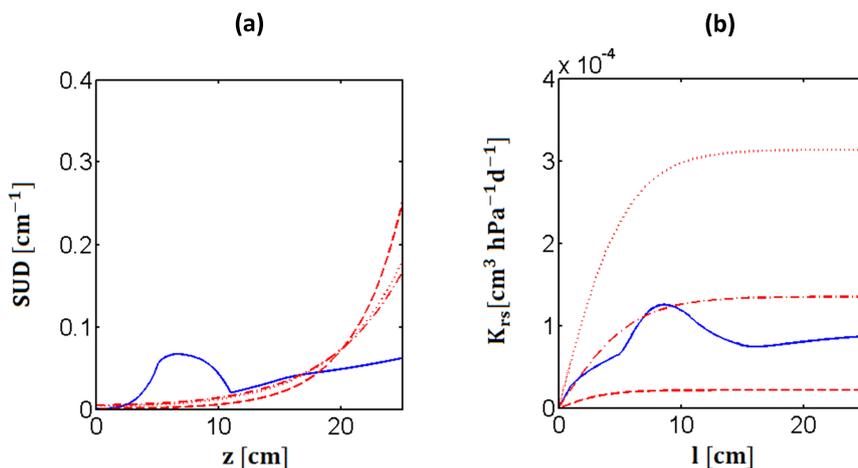
Figure 10. Macroscopic parameters: final SUD (a) and K_{rs} changes (b) for a growing maize lateral root branch with the local hydraulic properties estimated by Doussan et al. (1998b) (blue solid line) or the equivalent uniform roots (red lines) with minimal (dashed), maximal (dotted) or mean (dashed-dotted) hydraulic property values. The legend is the same as in the previous figure.

3.3 Properties of a growing root

When roots get older, their macroscopic hydraulic parameters vary not only because the root length increases but also because by root tissues changes by maturation. Maturation is defined here as the hydraulic property changes as a function of root age. This process is modelled by introducing root hydraulic properties depending on root age, such as:

5
$$
\begin{cases}
k_r = k_{r0} exp(-mt) \\
k_x = k_{x0} exp(mt)
\end{cases}
\tag{13}
$$

where $m\,[\mathrm{T}^{-1}]$ is the maturation rate. These equations are similar to the ones used in the exponential root hydraulic properties subsection (see Sect. A3) except that they define the properties as a function of time instead of distance to tip. We investigate here the sensitivity of growth and maturation processes on root macroscopic parameters. Figure 11 presents an analysis of the relative effects of maturation versus growth on the macroscopic properties of an ageing root system. We varied the root

10 parameters m and $\frac{v_0}{l_{max}}$ between 0.05 and 0.5 and between 0.01 and 0.1, respectively to investigate the impact of relative growth and maturation processes. Figure 11-a shows the integral of K_{rs} over time when simulating 40 days of growth and maturation of a root whose l_{max} is 10 cm. The numbers one to four represent extreme situations: fast growth and slow maturation (case 1), slow growth and maturation (case 2), fast growth and maturation (case 3) and slow growth and fast maturation (case 4), respectively. The conductances of these particular branches are plotted as a function of time in Fig. 11-b. They exhibit very

15 contrasted strategies. When the root growth is fast, the K_{rs} quickly reaches a high value. If the root maturation process is rapid, the final conductance is low. It can also be observed that the root properties change slowly when the root growth is low and rapidly when the root elongation rate is high. Figure 11-c plots the relative SUD (i.e., multiplied by root length) as a function of the relative root position z (i.e., divided by root length) after 20 days of growth. Again contrasted strategies appear with a maximal water uptake location at the root tip for cases 3 and 4 or at the root collar for cases 1 and 2. It is worth noting that a

20 constant elongation rate means a very small elongation rate to maximal root length ratio. So depending on the maturation rate, the constant elongation case rate is similar to case 2 or 4.

Figure 12 represents the effects of elongation rate on the root branch development (a) and its conductance (b). We consider a maize lateral root branch whose hydraulic properties are given by the two first subplots of Fig. 9 where the x-axis is now time and no more length. It corresponds to the hydraulic properties calculated by Doussan et al. (1998b). Coupling the intrinsic axial

25 conductance and radial conductivity transition ages, we obtain six different stretches in addition to the isolated distal region. From the tip to the collar: linear k_x (between 0 and 5 days), linear k_r and k_x (5-7), linear k_x (7-11), uniform root (11-15), linear k_r (15-18) and uniform (18-...). Each zone between two successive transition ages has its own colour from dark blue to orange. The maximal root length is 10 cm and four elongation rates are computed: $0.5cm/d$ (dotted lines in both panel and for all curves), $1cm/d$ (dashed-dotted lines), $1.5cm/d$ (dashed lines) and $2cm/d$ (solid lines).

30 In subplot (a) are shown both the total root branch length (black lines) and the stretch lengths (from the dark blue to the oranges lines, representing respectively the stretches from the tip to the root collar). At any time the sum of the stretch lengths is to the total root branch length. From its origination time, each single root stretch appears, reaches a maximal value

(a)   **(b)**   **(c)**
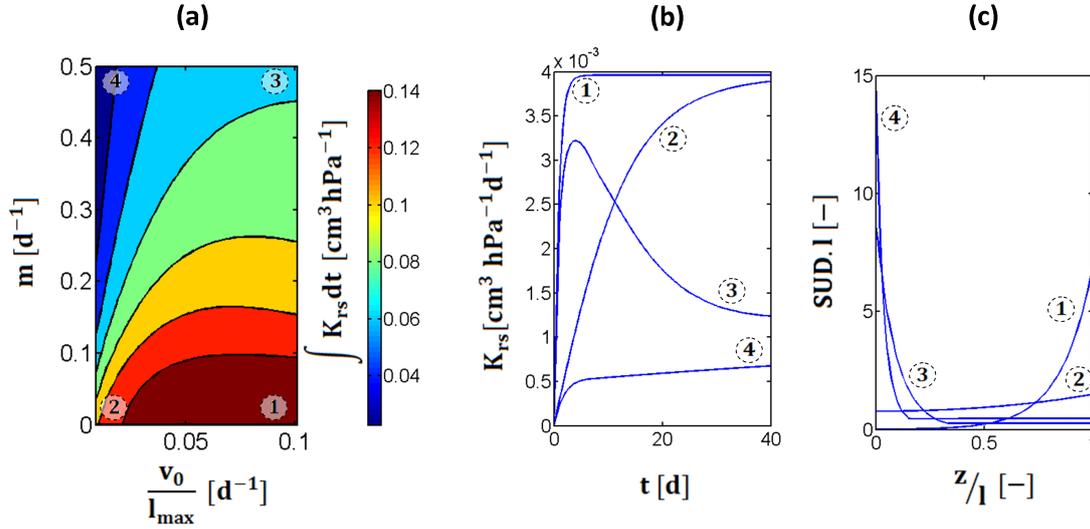
Figure 11. Integral of the root conductance over time when changing the elongation rate $\frac{v_0}{l_{max}}$ (x-axis) and the maturation rate m (y-axis) (a). Root hydraulic conductances of the four extreme cases numbered and indicated in (a) as a function of time (b). Relative uptake of the four branches after 20 days as a function of the relative position to the root tip (l is the root branch length and $z = 0$ at the tip) (c).

and then decreases. The maximal value of each zone is reached when arrives the consecutive transition time. In subplot (b) are represented the root branch conductance K_{rs} and the effect of changing the initial elongation rate on this macroscopic parameter.

3.4 Optimal geometric properties

5 The new solutions of the water flow equation are key to estimate optimal geometric properties of root branches. As an illustration we may want to maximize the root branch conductance K_{rs} of uniform roots and compare the results with those of roots with varying hydraulic property profiles. Using a carbon cost as a constraint, it writes:

maximize $K_{rs}(r,l)$ subject to $V_0 = \pi r^2 l$

where $V_0\,[L^3]$ is the volume constraint. To solve this optimization problem we use Lagrange multipliers λ. We define a new
10 function L:

$$L(r,l,\lambda) = K_{rs}(r,l) + \lambda\left(\pi r^2 l - V_0\right)$$

whose maximum is found when:
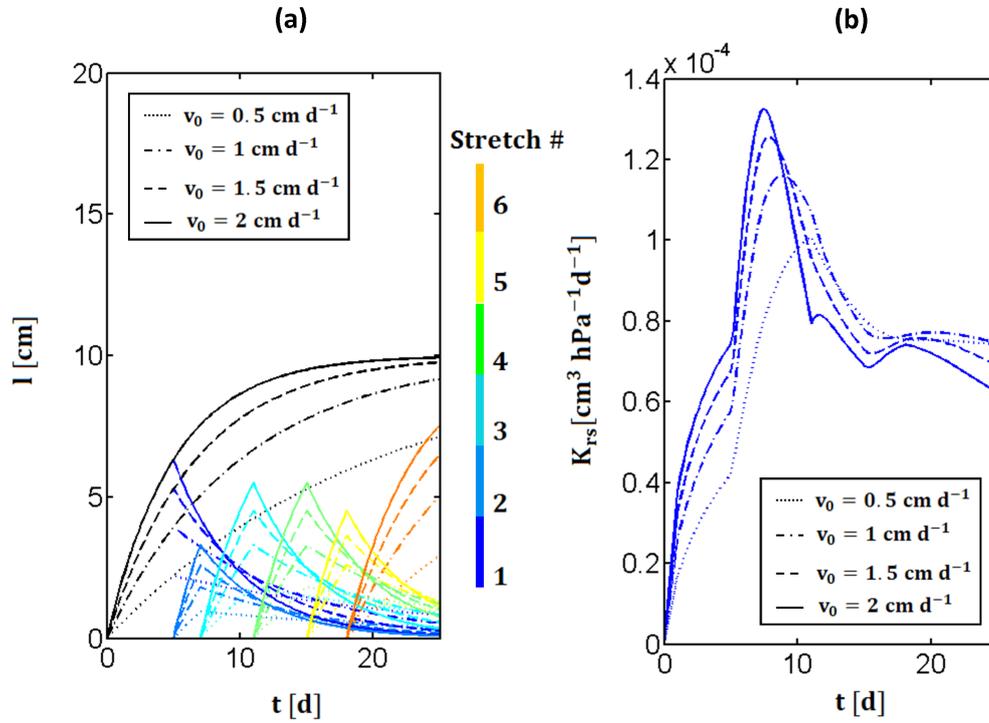
Figure 12. Total root branch length (black line), root stretch lengths (from dark blue to orange lines, representing respectively stretches from the tip to the collar) (a) and root branch conductance K_{rs} as a function of time (b). Lengths and conductances are computed for four different initial elongation rates: $0.5 cm/d$ (dotted lines), $1cm/d$ (dashed-dotted lines), $1.5cm/d$ (dashed lines) and $2cm/d$ (solid lines).

$$\nabla_{r,l,\lambda} L = 0$$

The previous equation is equivalent to:

$$\begin{cases} l\frac{\partial K_{rs}}{\partial r} + 2\lambda\pi rl = 0 \\ \frac{\partial K_{rs}}{\partial l} + \lambda\pi r^2 l = 0 \\ V_0 = \pi r^2 l \end{cases} \tag{14}$$

Using appropriate equations to calculate the root conductance, we find an optimal radius and length that maximize root
5   water uptake. As an illustration, we compare the optimal root radius of a root with uniform and constant hydraulic properties,

Hydrology and
Earth System
Sciences

Discussions

EGU

Open Access

a root whose uniform root properties depend on the root radius (Biondini, 2008) and a root whose hydraulic properties vary exponentially along the root axis. Mathematically, it writes, respectively:

$$
\begin{cases}
\text{Uniform } k_r \text{ and } k_x : k_r(z) = k_{r0} \text{ and } k_x(z) = k_{x0} \\
\text{Uniform } k_r(r) \text{ and } k_z(r) : k_r(r) = k_{r0}\frac{r_0}{r} \text{ and } k_x(r) = \frac{b\pi}{8\mu}r^5 \\
\text{Exponential } k_r \text{ and } k_z : k_r(z) = \gamma_2 exp(-\beta_2 z) \text{ and } k_r(z) = \gamma_2 exp(-\beta_2 z)
\end{cases}
\tag{15}
$$

The parametrization for the exponential root and the uniform root whose hydraulic properties depend on the root radius come respectively from Zarebanadkouki et al. (2016) and Biondini (2008). The uniform hydraulic properties of the first root are the mean values of the exponential conductivities evaluated for optimal geometric parameters. The root conductances of the three cases are shown in Fig. 13 for a volume constraint of 0.05 cm^3: the dashed line is the uniform root, the dotted line is the uniform root whose hydraulic properties depend on the root radius and the solid one is the root with exponential hydraulic property profiles. The red stars point the optimal radii.
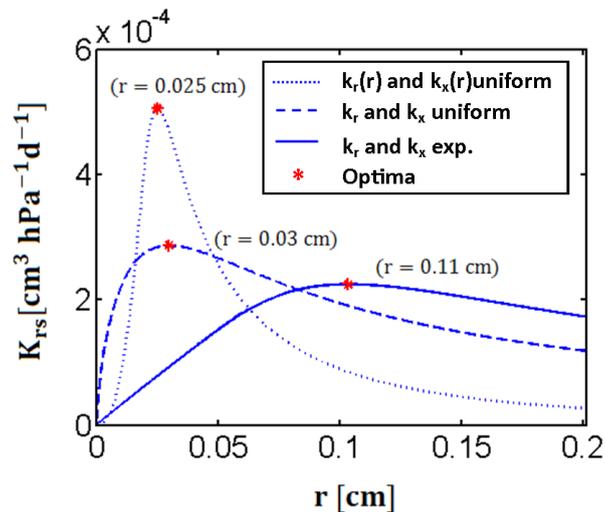
Figure 13. Root branch conductance as a function of root branch radius under a constant volume constraint for a uniform root whose hydraulic properties depend on the root radius (dotted line), a uniform root (dashed line) and a root with exponential conductivity profiles (solid line). The red stars point the optimal radii (i.e., that maximize the root branch conductance).

Unlike previous approaches (Biondini, 2008; Roose and Schnepf, 2008) we consider here that the hydraulic properties may be intrinsic functions of the root tissues and do not necessarily depend on the root radius. As highlighted by the red stars, the optimal root radii vary considerably when integrating this concept: from 0.025 cm for the uniform profile (varying according to the root radius) to 0.11 cm for the exponential root. We find that optimal roots have a larger radius and therefore a shorter length when presenting exponential conductivity profiles.

4 Conclusions

Six new solutions of the water flow equation in root branches are presented in addition to the uniform root of Landsberg and Fowkes (1978). In the newly considered cases the root hydraulic properties vary as a function of the distance to root tip. When the radial conductivity and the intrinsic axial conductance change linearly or exponentially alone or in combination, exact

5   solutions of the xylem potential and water flow inside the root exist. They were used to calculate the macroscopic parameters of the corresponding root branches. Moreover they were associated to make complex root branches of changing root hydraulic property profiles as observed in nature or combined with an elongation rate to obtain the root macroscopic parameters and uptake profile as a function of root age. As illustrated these complex functions were not well represented by root of equivalent but uniform root hydraulic properties.

10   Considering these changes in hydraulic properties along roots also enabled us investigating the effects of root maturation or root tissue development and differentiation on root water uptake. This gave interesting perspectives to evaluate both growth and maturation and their combined effects on root water uptake. The obtained analytical solutions allowed us to assess the impact of changing axial or radial conductivity along a root branch on root water uptake. These changes can be linked to dynamics of root growth and root tissue maturation so that different strategies of growth and maturation dynamics, e.g. rapid growth and

15   slow maturation *versus* slow growth and rapid maturation, were investigated using these analytical functions.

These solutions were also used to define optimal root branch geometrical parameters for water uptake. Indeed, Landsberg and Fowkes (1978) model has been used for decades to define optimal root systems in terms of water uptake subject to minimal carbon cost (Biondini, 2008). Using the water uptake solution developed in their manuscript, one typically observes a monotonic behaviour of root water uptake capacity with root length. The use of such a model also typically implies that, for a

20   uniform root in a uniform soil water potential, the uptake increases monotonically towards the proximal end. This is no more systematically the case with the newly developed solutions. When considering variations in hydraulic properties along a root axis, which typically correspond with an increase in axial and a decrease in radial conductivity with distance to root tip, the analytical solutions that account for these changes revealed considerably different behaviours. The root effective conductance may increase with root length more steadily than in case of a uniform root or even decrease with root length. Similarly with

25   the newly developed solutions, the maximal water uptake location was no more located at root proximal end. Non-monotonic functions of root water uptake emerged from the new solutions. Therefore, the search for optimal root systems should also account for variations of root properties along roots.

The new models will be combined as building blocks to generate complete root system hydraulic architectures defining plant genotypes in order to compare plant performances in contrasted environments using soil-root-atmosphere continuum model

30   such as R-SWMS (Javaux et al., 2008).

5 Code availability

The code is available and can be freely shared.

6 Data availability

Not applicable

References

Alm, D. M., Cavelier, J., and Nobel, P. S.: A Finite-element Model of Radial and Axial Conductivities for Individual Roots: Development and Validation for Two Desert Succulents, Annals of Botany, 69, 87–92, 1992.

Biondini, M.: Allometric scaling laws for water uptake by plant roots, Journal of Theoretical Biology, 251, 35–59, doi:10.1016/j.jtbi.2007.11.018, http://linkinghub.elsevier.com/retrieve/pii/S0022519307005784, 2008.

Bramley, H., Turner, N. C., Turner, D. W., and Tyerman, S. D.: Comparison between gradient-dependent hydraulic conductivities of roots using the root pressure probe: the role of pressure propagations and implications for the relative roles of parallel radial pathways, Plant, Cell & Environment, 30, 861–874, doi:10.1111/j.1365-3040.2007.01678.x, http://doi.wiley.com/10.1111/j.1365-3040.2007.01678.x, 2007.

Campos, H., Cooper, M., Habben, J., Edmeades, G., and Schussler, J.: Improving drought tolerance in maize: a view from industry, Field Crops Research, 90, 19–34, doi:10.1016/j.fcr.2004.07.003, http://www.sciencedirect.com/science/article/pii/S0378429004001571, 2004.

Cattivelli, L., Rizza, F., Badeck, F.-W., Mazzucotelli, E., Mastrangelo, A. M., Francia, E., Marè, C., Tondelli, A., and Stanca, A. M.: Drought tolerance improvement in crop plants: An integrated view from breeding to genomics, Field Crops Research, 105, 1–14, doi:10.1016/j.fcr.2007.07.004, http://www.sciencedirect.com/science/article/pii/S0378429007001414, 2008.

Chaumont, F. and Tyerman, S. D.: Aquaporins: Highly Regulated Channels Controlling Plant Water Relations, PLANT PHYSIOLOGY, 164, 1600–1618, doi:10.1104/pp.113.233791, http://www.plantphysiol.org/cgi/doi/10.1104/pp.113.233791, 2014.

Couvreur, V., Vanderborght, J., and Javaux, M.: A simple three-dimensional macroscopic root water uptake model based on the hydraulic architecture approach, Hydrology and Earth System Sciences, 16, 2957–2971, doi:10.5194/hess-16-2957-2012, http://www.hydrol-earth-syst-sci.net/16/2957/2012/, 2012.

Couvreur, V., Vanderborght, J., Beff, L., and Javaux, M.: Horizontal soil water potential heterogeneity: simplifying approaches for crop water dynamics models, Hydrology and Earth System Sciences, 18, 1723–1743, doi:10.5194/hess-18-1723-2014, http://www.hydrol-earth-syst-sci.net/18/1723/2014/, 2014.

Doussan, C., Pagès, L., and Vercambre, G.: Modelling of the Hydraulic Architecture of Root Systems: An Integrated Approach to Water Absorption—Model Description, Annals of Botany, 81, 213–223, doi:10.1006/anbo.1997.0540, http://aob.oxfordjournals.org/cgi/doi/10.1006/anbo.1997.0540, 1998a.

Doussan, C., Vercambre, G., and Pagès, L.: Modelling of the hydraulic architecture of root systems: An integrated approach to water absorption—distribution of axial and radial conductances in maize, Annals of Botany, 81, 225–232, http://aob.oxfordjournals.org/content/81/2/225.short, 1998b.

Enstone, D. E., Peterson, C. A., and Ma, F.: Root Endodermis and Exodermis: Structure, Function, and Responses to the Environment, Journal of Plant Growth Regulation, 21, 335–351, doi:10.1007/s00344-003-0002-2, http://link.springer.com/10.1007/s00344-003-0002-2, 2002.

Frensch, J. and Steudle, E.: Axial and radial hydraulic resistance to roots of maize (Zea mays L.), Plant Physiology, 91, 719–726, http://www.plantphysiol.org/content/91/2/719.short, 1989a.

Frensch, J. and Steudle, E.: Axial and Radial Hydraulic Resistance to Roots of Maize (Zea mays L.) 1, Plant Physiology, 91, 719–726, http://www.ncbi.nlm.nih.gov/pmc/articles/PMC1062061/, 1989b.

Frensch, J., Hsiao, T. C., and Steudle, E.: Water and solute transport along developing maize roots, Planta, 198, 348–355, doi:10.1007/BF00620050, http://link.springer.com/10.1007/BF00620050, 1996.

Hachez, C., Moshelion, M., Zelazny, E., Cavez, D., and Chaumont, F.: Localization and Quantification of Plasma Membrane Aquaporin Expression in Maize Primary Root: A Clue to Understanding their Role as Cellular Plumbers, Plant Molecular Biology, 62, 305–323, doi:10.1007/s11103-006-9022-1, http://link.springer.com/10.1007/s11103-006-9022-1, 2006.

Javaux, M., Schröder, T., Vanderborght, J., and Vereecken, H.: Use of a three-dimensional detailed modeling approach for predicting root water uptake, Vadose Zone Journal, 7, 1079–1088, http://vzj.geoscienceworld.org/content/7/3/1079.short, 2008.

Landsberg, J. J. and Fowkes, N. D.: Water Movement Through Plant Roots, Annals of Botany, 42, 493–508, doi:10.1093/oxfordjournals.aob.a085488, http://aob.oxfordjournals.org/content/42/3/493, 1978.

Leitner, D., Meunier, F., Bodner, G., Javaux, M., and Schnepf, A.: Impact of contrasted maize root traits at flowering on water stress tolerance – A simulation study, Field Crops Research, doi:10.1016/j.fcr.2014.05.009, http://linkinghub.elsevier.com/retrieve/pii/S037842901400135X, 2014.

Lobet, G., Couvreur, V., Meunier, F., Javaux, M., and Draye, X.: Plant Water Uptake in Drying Soils, Plant Physiology, doi:10.1104/pp.113.233486, http://www.plantphysiol.org/cgi/doi/10.1104/pp.113.233486, 2014.

Martre, P., Durand, J.-L., and Cochard, H.: Changes in axial hydraulic conductivity along elongating leaf blades in relation to xylem maturation in tall fescue, New Phytologist, 146, 235–247, doi:10.1046/j.1469-8137.2000.00641.x, http://onlinelibrary.wiley.com/doi/10.1046/j.1469-8137.2000.00641.x/abstract, 2000.

McElrone, A. J., Choat, B., Gambetta, G. A., and Brodersen, C. R.: Water Uptake and Transport in Vascular Plants, Nature Education Knowledge, 5, 6, 2013.

Meunier, F., Couvreur, V., Draye, X., Vanderborght, J., and Javaux, M.: Towards quantitative root hydraulic phenotyping: Novel mathematical functions to calculate plant-scale hydraulic parameters from root system functional and structural traits, Submitted to Journal of Mathematical biology, Submitted.

Newman, E. I.: Water Movement Through Root Systems, Philosophical Transactions of the Royal Society B: Biological Sciences, 273, 463–478, doi:10.1098/rstb.1976.0025, http://rstb.royalsocietypublishing.org/cgi/doi/10.1098/rstb.1976.0025, 1976.

Pagès, L., Vercambre, G., Drouet, J. L., Lecompte, F., Collet, C., and Le Bot, J.: Root Typ: a generic model to depict and analyse the root system architecture, Plant and Soil, 258, 103–119, http://www.springerlink.com/index/R742L256T7142875.pdf, 2004.

Passioura, J. B.: The transport of water from soil to shoot in wheat seedlings, Journal of Experimental Botany, 31, 333–345, http://jxb.oxfordjournals.org/content/31/1/333.short, 1980.

Roose, T. and Schnepf, A.: Mathematical models of plant–soil interaction, Philosophical Transactions of the Royal Society A: Mathematical, Physical and Engineering Sciences, 366, 4597–4611, http://rsta.royalsocietypublishing.org/content/366/1885/4597.abstract, 2008.

Steudle, E.: Water uptake by roots: effects of water deficit, Journal of Experimental Botany, 51, 1531–1542, doi:10.1093/jexbot/51.350.1531, http://jxb.oxfordjournals.org/content/51/350/1531, 2000.

Steudle, E. and Peterson, C. A.: How does water get through roots?, Journal of Experimental Botany, 49, 775–788, doi:10.1093/jxb/49.322.775, http://jxb.oxfordjournals.org/content/49/322/775, 1998.

Varney, G. T. and Canny, M. J.: Rates of water uptake into the mature root system of maize plants, New Phytologist, 123, 775–786, doi:10.1111/j.1469-8137.1993.tb03789.x, http://doi.wiley.com/10.1111/j.1469-8137.1993.tb03789.x, 1993.

Volpe, V., Marani, M., Albertson, J., and Katul, G.: Root controls on water redistribution and carbon uptake in the soil–plant system under current and future climate, Advances in Water Resources, 60, 110–120, doi:10.1016/j.advwatres.2013.07.008, http://linkinghub.elsevier.com/retrieve/pii/S0309170813001231, 2013.

Zarebanadkouki, M., Meunier, F., Couvreur, V., Cesar, J., Javaux, M., and Carminati, A.: Estimation of the hydraulic conductivities of lupine roots by inverse modelling of high-resolution measurements of root water uptake, Annals of Botany, p. mcw154, doi:10.1093/aob/mcw154, http://aob.oxfordjournals.org/lookup/doi/10.1093/aob/mcw154, 2016.

Zwieniecki, M. A., Thompson, M. V., and Holbrook, N. M.: Understanding the Hydraulics of Porous Pipes: Tradeoffs Between Water Uptake
5   and Root Length Utilization, Journal of Plant Growth Regulation, 21, 315–323, doi:10.1007/s00344-003-0008-9, http://link.springer.com/10.1007/s00344-003-0008-9, 2002.

Table 1. Local hydraulic properties $k_r(z)$ and $k_x(z)$ for the different cases.

	$\mathbf{k_r(z)}$	$\mathbf{k_x(z)}$
Uniform root	$k_r(z) = k_{r0}$	$k_x(z) = k_{x0}$
Linear k_r	$k_r(z) = a_0 z + b_0$	$k_x(z) = k_{x0}$
Linear k_x	$k_r(z) = k_{r0}$	$k_x(z) = c_0 z + d_0$
Linear k_r and k_x	$k_r(z) = a_0 z + b_0$	$k_x(z) = c_0 z + d_0$
Exponential k_r	$k_r(z) = \gamma_2 exp(-\beta_2 z)$	$k_x(z) = k_{x0}$
Exponential k_x	$k_r(z) = k_{r0}$	$k_x(z) = \gamma_1 exp(\beta_1 z)$
Exponential k_r and k_x	$k_r(z) = \gamma_2 exp(-\beta_2 z)$	$k_x(z) = \gamma_1 exp(\beta_1 z)$

Table 2. Local hydraulic property function parameters, their units, the expression of adjusted parameters and their corresponding units.

Parameter	Unit	Adjusted parameter	Unit
k_{r0}	$LT^{-1}P^{-1}$		
k_{x0}	$L^4T^{-1}P^{-1}$		
a_0	$T^{-1}P^{-1}$	$a = 2\pi r a_0$	$LT^{-1}P^{-1}$
b_0	$LT^{-1}P^{-1}$	$b = 2\pi r b_0$	$L^2T^{-1}P^{-1}$
c_0	$L^3T^{-1}P^{-1}$	$c = \frac{c_0}{2\pi r k_{r0}}$	L
d_0	$L^4T^{-1}P^{-1}$	$d = \frac{d_0}{2\pi r k_{r0}}$	L^2
γ_1	$L^4T^{-1}P^{-1}$	$\gamma_r = \frac{2\pi r \gamma_2}{k_{x0}}$	L^{-2}
γ_2	$LT^{-1}P^{-1}$	$\gamma_x = \frac{2\pi r k_{r0}}{\gamma_1}$	L^{-2}
β_1	L^{-1}	$\gamma = 2\pi r \frac{\gamma_2}{\gamma_1}$	L^{-2}
β_2	L^{-1}	$\beta = \beta_1 + \beta_2$	L^{-1}

Hydrology and
Earth System
Sciences

Open Access

Discussions

EGU

Table 3. Linearly independent functions f_1 and f_2 according to the considered local root hydraulic properties.

	$\mathbf{f_1(z)}$	$\mathbf{f_2(z)}$
Uniform root	$cosh(\tau z)$	$sinh(\tau z)$
Linear k_r	$Ai\left(\dfrac{az+b}{a^{\frac{2}{3}}k_{x0}^{\frac{1}{3}}}\right)$	$Bi\left(\dfrac{az+b}{a^{\frac{2}{3}}k_{x0}^{\frac{1}{3}}}\right)$
Linear k_x	$\sqrt{\dfrac{2}{c}}I_0\left(2\sqrt{\dfrac{d+cz}{c^2}}\right)$	$\sqrt{\dfrac{2}{c}}K_0\left(2\sqrt{\dfrac{d+cz}{c^2}}\right)$
Linear k_r and k_x	$exp\left(-\dfrac{\sqrt{a}z}{\sqrt{c_0}}\right)M\left(\dfrac{\sqrt{a}c_0^{3/2}+bc_0-ad_0}{2\sqrt{a}c_0^{3/2}},1,\dfrac{2\sqrt{a}(c_0z+d_0)}{c^{3/2}}\right)$	$exp\left(-\dfrac{\sqrt{a}z}{\sqrt{c_0}}\right)U\left(\dfrac{-\sqrt{a}c_0^{3/2}-bc_0+ad_0}{2\sqrt{a}c_0^{3/2}},1,\dfrac{2\sqrt{a}(c_0z+d_0)}{c^{3/2}}\right)$
Exponential k_r	$I_0\left(\dfrac{2\sqrt{\gamma_r exp(-\beta_2 z)}}{\beta2}\right)$	$K_0\left(\dfrac{2\sqrt{\gamma_r exp(-\beta_2 z)}}{\beta2}\right)$
Exponential k_x	$\dfrac{\sqrt{\gamma_x exp(-\beta_1 z)}}{\beta_1}I_1\left(\dfrac{2\sqrt{\gamma_x exp(-\beta_1 z)}}{\beta_1}\right)$	$\dfrac{\sqrt{\gamma_x exp(-\beta_1 z)}}{\beta_1}K_1\left(\dfrac{2\sqrt{\gamma_x exp(-\beta_1 z)}}{\beta_1}\right)$
Exponential k_r and k_x	$\beta^{-\frac{\beta_1}{\beta}}\gamma^{\frac{\beta_1}{2\beta}}(exp(-\beta z))^{\frac{\beta_1}{2\beta}}\Gamma\left(1-\frac{\beta_1}{\beta}\right)I_{-\frac{\beta_1}{\beta}}\left(\dfrac{2\sqrt{exp(-\beta z)\gamma}}{\beta}\right)$	$\beta^{-\frac{\beta_1}{\beta}}\gamma^{\frac{\beta_1}{2\beta}}(exp(-\beta z))^{\frac{\beta_1}{2\beta}}\Gamma\left(1+\frac{\beta_1}{\beta}\right)I_{\frac{\beta_1}{\beta}}\left(\dfrac{2\sqrt{exp(-\beta z)\gamma}}{\beta}\right)$

Appendix A: New solutions of the root water flow equation

In this appendix, we provide detailed solutions of the water flow equation when the root hydraulic properties are uniform (Landsberg and Fowkes, 1978) or when they vary linearly or exponentially, alone or together along the root axis. These solutions of the water flow equation (4) have been obtained using the symbolic calculation toolbox of Matlab. All solutions are

5   summarized in Table 3.

A1   Uniform root hydraulic properties

The solution of the water flow equation in a uniform root has been proposed by Landsberg and Fowkes (1978). We present their methodology and principal results in this section to illustrate with the simplest case how to derive the water flow equation solution and the macroscopic parameters.

10   The simplest root is made of uniform root properties: intrinsic axial conductance k_{x0} $[\mathrm{L^4 T^{-1} P^{-1}}]$ and radial conductivity k_{r0} $[\mathrm{L T^{-1} P^{-1}}]$:

$$
\begin{cases}
k_r(z) = k_{r0} \\
k_x(z) = k_{x0}
\end{cases}
$$

Equation (4) becomes:

$$
k_{x0} \frac{d^2 \Psi_x(z)}{dz^2} = 2\pi r k_{r0} \left(\Psi_x(z) - \Psi_{soil} \right)
$$

15   The general solution of this differential equation is given in terms of hyperbolic sinus and cosinus:

$$
\Psi_x(z) = \Psi_{soil} + c_1 cosh(\tau z) + c_2 sinh(\tau z) \tag{A1}
$$

where we define τ $[\mathrm{L^{-1}}]$:

$$
\tau = \sqrt{\frac{2\pi r k_{r0}}{k_{x0}}}
$$

Here, the independent functions $f_1(z)$ and $f_2(z)$ are thus $cosh(\tau z)$ and $sinh(\tau z)$.

20   The coefficients are obtained for the bottom no-flux boundary conditions in case of single stretch root branch (see Appendix C and particularly Eq. (C1)):

$$
\begin{cases}
c_1^{nf} = \frac{\Psi_{collar} - \Psi_{soil}}{cosh(\tau l)} \\
c_2^{nf} = 0
\end{cases}
$$

Here and in the following, the superscript nf stands for non-flux. Using these coefficients, we find the general solution of the xylem water potential profile:

$$\Psi_x^{nf}(z) = \Psi_{soil} + (\Psi_{collar} - \Psi_{soil}) \frac{cosh(\tau z)}{cosh(\tau l)}$$

The axial flow is then obtained using Eq. (3)

5 $$J_x^{nf}(z) = -\kappa (\Psi_{collar} - \Psi_{soil}) \frac{sinh(\tau z)}{cosh(\tau l)}$$

And the macroscopic parameters are derived thanks to Eq. (C4)

$$K_{rs}^{nf}(l) = \kappa tanh(\tau l)$$

$$SUD^{nf}(z) = \tau \frac{cosh(\tau z)}{sinh(\tau l)}$$

10 where tanh is the hyperbolic tangent and $\kappa \, [\mathrm{L^3 T^{-1} P^{-1}}]$ is the asymptotic root conductance defined by:

$$\kappa = k_{x0}\tau$$

For the bottom flux boundary condition (6) (solution for a root branch with multiple stretches), the coefficients are:

$$\begin{cases} c_1 = (\Psi_{proximal,i} - \Psi_{soil}) \left(\frac{\kappa}{\kappa cosh(\tau l_i) + K_{rs,i-1} sinh(\tau l_i)} \right) \\ c_2 = (\Psi_{proximal,i} - \Psi_{soil}) \left(\frac{K_{rs,i-1}}{\kappa cosh(\tau l_i) + K_{rs,i-1} sinh(\tau l_i)} \right) \end{cases}$$

And the solution of the water flow equation in the root becomes:

15 $$\Psi_x(z) = \Psi_{soil} + (\Psi_{proximal,i} - \Psi_{soil}) \frac{\kappa cosh(\tau z) + K_{rs,i-1} sinh(\tau z)}{\kappa cosh(\tau l_i) + K_{rs,i-1} sinh(\tau l_i)}$$

which leads to the following axial flow:

$$J_x(z) = -\kappa (\Psi_{proximal,i} - \Psi_{soil}) \frac{\kappa sinh(\tau z) + K_{rs,i-1} cosh(\tau z)}{\kappa cosh(\tau l_i) + K_{rs,i-1} sinh(\tau l_i)}$$

The macroscopic parameters become:

$$K_{rs,i}(l_i) = \kappa \left(\frac{\kappa sinh(\tau l_i) + K_{rs,i-1} cosh(\tau l_i)}{\kappa cosh(\tau l_i) + K_{rs,i-1} sinh(\tau l_i)} \right)$$

Hydrology and
Earth System
Sciences

Discussions

Open Access

$$SUD_i(z) = \tau \left(\frac{\kappa cosh(\tau z) + K_{rs,i-1} sinh(\tau z)}{\kappa sinh(\tau l_i) + K_{rs,i-1} cosh(\tau l_i)} \right)$$

The flux boundary solutions are a generalization of the non-flux solutions as they converge towards the same results as $K_{rs,i-1} \to 0$.

5 A2 Linear root hydraulic property profiles

In case of roots with linear hydraulic property profiles, different cases are distinguished and are investigated successively.

A2.1 Linear k_r

Equation (4) can be solved with different root linear hydraulic property profiles. Let us consider a uniform intrinsic axial conductance and a radial conductivity varying linearly along the root:

$$\begin{cases} k_r(z) = a_0 z + b_0 \\ k_x(z) = k_{x0} \end{cases}$$

10

where $a_0 \, [\mathrm{T^{-1}P^{-1}}]$ and $b_0 \, [\mathrm{LT^{-1}P^{-1}}]$ are shape parameters.

Equation (4) yields:

$$k_{x0} \frac{d^2 \Psi_x(z)}{dz^2} = 2\pi r (a_0 z + b_0) \left(\Psi_x(z) - \Psi_{soil} \right)$$

and can be rewritten as:

15

$$\frac{d^2 \Psi_x(z)}{dz^2} = \frac{(az + b)}{k_{x0}} \left(\Psi_x(z) - \Psi_{soil} \right)$$

where we have defined:

$$\begin{cases} a = 2\pi r a_0 \\ b = 2\pi r b_0 \end{cases}$$

with $a \, [\mathrm{LT^{-1}P^{-1}}]$ and $b \, [\mathrm{L^2 T^{-1}P^{-1}}]$ the revised shape parameters. The general solution of this differential equation is now:

$$\Psi_x(z) = \Psi_{soil} + c_1 Ai\left(\frac{az + b}{a^{\frac{2}{3}} k_{x0}^{\frac{1}{3}}} \right) + c_2 Bi\left(\frac{az + b}{a^{\frac{2}{3}} k_{x0}^{\frac{1}{3}}} \right) \tag{A2}$$

20

where c_1 and c_2 can anew be obtained using boundary conditions. Ai and Bi are the Airy functions of the first and second kind, respectively. It is worth noting that we obtain a similar solution if the root radius changes linearly along the root while k_x remains constant.

A2.2   Linear k_x

If the root intrinsic axial conductance varies while the radial conductivity is uniform, i.e.:

$$\begin{cases} k_r(z) = k_{r0} \\ k_x(z) = c_0 z + d_0 \end{cases}$$

with $c_0 \left[\mathrm{L^3 T^{-1} P^{-1}}\right]$ and $d_0 \left[\mathrm{L^4 T^{-1} P^{-1}}\right]$ the shape parameters, the general water flow Eq. (4) yields:

5   $(c_0 z + d_0)\dfrac{d^2 \Psi_x(z)}{dz^2} + c_0 \dfrac{d\Psi_x(z)}{dz} = 2\pi r k_r \left(\Psi_x(z) - \Psi_{soil}\right)$

Again we rewrite the equation as:

$(cz + d)\dfrac{d^2 \Psi_x(z)}{dz^2} + c\dfrac{d\Psi_x(z)}{dz} = \left(\Psi_x(z) - \Psi_{soil}\right)$

with the following definitions of the revised shape parameters:

$$\begin{cases} c = \frac{c_0}{2\pi r k_{r0}} \\ d = \frac{d_0}{2\pi r k_{r0}} \end{cases}$$

10   The units of c and d are $[\mathrm{L}]$ and $[\mathrm{L^2}]$, respectively. The general solution becomes:

$$\Psi_x(z) = \Psi_{soil} + \sqrt{\frac{2}{c}}\left(c_1 I_0\left(2\sqrt{\frac{d+cz}{c^2}}\right) + c_2 K_0\left(2\sqrt{\frac{d+cz}{c^2}}\right)\right) \tag{A3}$$

I_ν and K_ν are the modified Bessel function of the first and second kind of order ν ($\nu = 0$, here), respectively.

A2.3   Linear k_r and k_x

We assume now a linear relation between the hydraulic properties and the distance to the tip:

15   $$\begin{cases} k_r(z) = a_0 z + b_0 \\ k_x(z) = c_0 z + d_0 \end{cases}$$

The water flow equation becomes:

$(c_0 z + d_0)\dfrac{d^2 \Psi_x(z)}{dz^2} + c_0 \dfrac{d\Psi_x(z)}{dz} = 2\pi r (a_0 z + b_0)\left(\Psi_x(z) - \Psi_{soil}\right)$

After rewriting the parameters it yields:

$$(c_0 z + d_0)\frac{d^2\Psi_x(z)}{dz^2} + c_0\frac{d\Psi_x(z)}{dz} = (az+b)\left(\Psi_x(z) - \Psi_{soil}\right)$$

This equation has now the general solution:

$$\Psi_x(z) = \Psi_{soil} + exp\left(-\frac{\sqrt{a}z}{\sqrt{c_0}}\right)$$

$$\left(c_1 M\left(\frac{\sqrt{a}c_0^{3/2} + bc_0 - ad_0}{2\sqrt{a}c_0^{3/2}}, 1, \frac{2\sqrt{a}(c_0 z + d_0)}{c^{3/2}}\right) + c_2 U\left(\frac{-\sqrt{a}c_0^{3/2} - bc_0 + ad_0}{2\sqrt{a}c_0^{3/2}}, 1, \frac{2\sqrt{a}(c_0 z + d_0)}{c^{3/2}}\right)\right) \quad \text{(A4)}$$

with M and U the confluent hypergeometric function of the first and second kind, respectively.

A3 Exponential root hydraulic property profiles

Let us finally consider a root whose root hydraulic properties vary exponentially along the root axis:

$$\begin{cases} k_x(z) = \gamma_1 exp(\beta_1 z) \\ k_r(z) = \gamma_2 exp(-\beta_2 z) \end{cases}$$

with $\gamma_1\,[\mathrm{L^4 T^{-1} P^{-1}}]$, $\beta_1\,[\mathrm{L^{-1}}]$, $\gamma_2\,[\mathrm{LT^{-1}P^{-1}}]$ and $\beta_2\,[\mathrm{L^{-1}}]$ are shape parameters.

The water flow equation becomes:

$$\frac{\partial^2\Psi_x(z)}{\partial z^2} + \beta_1\frac{\partial\Psi_x(z)}{\partial z} = \gamma exp(-\beta z)\left(\Psi_x(z) - \Psi_{soil}\right)$$

with $\gamma = 2\pi r\frac{\gamma_2}{\gamma_1}\,[\mathrm{L^{-2}}]$ and $\beta = \beta_1 + \beta_2\,[\mathrm{L^{-1}}]$.

Solutions of this differential equation are of type:

$$\Psi_x(z) = \Psi_{soil} + \beta^{-\frac{\beta_1}{\beta}}\gamma^{\frac{\beta_1}{2\beta}}\left(exp(-\beta z)\right)^{\frac{\beta_1}{2\beta}}$$

$$\left[c_1\Gamma\left(1 - \frac{\beta_1}{\beta}\right)I_{-\frac{\beta_1}{\beta}}\left(\frac{2\sqrt{exp(-\beta z)\gamma}}{\beta}\right) + c_2\Gamma\left(1 + \frac{\beta_1}{\beta}\right)I_{\frac{\beta_1}{\beta}}\left(\frac{2\sqrt{exp(-\beta z)\gamma}}{\beta}\right)\right] \quad \text{(A5)}$$

with Γ the gamma function.

The cases of mixed uniform/exponential hydraulic property may be easily solved using the same methodology.

Appendix B: Macroscopic parameters

To calculate the general form of the macroscopic parameters defined as:

$$\begin{cases} K_{rs,i} = \frac{J_x(l_i)}{\Psi_{soil} - \Psi_x(l_i)} \\ SUD_i(z) = \frac{q_r(z)}{J_x(l_i)} \end{cases} \tag{B1}$$

we need to combine combining Eq. (3) and (5) with the root stretch boundary conditions (6). The two unknowns, $c_{1,i}$ and

5    $c_{2,i}$, are given, in matrix notation, by:

$$\begin{bmatrix} -k_x(l_{i-1})f'_{1,i}(l_{i-1}) & -k_x(l_{i-1})f'_{2,i}(l_{i-1}) \\ f_{1,i}(l_i) & f_{2,i}(l_i) \end{bmatrix} \begin{bmatrix} c_{1,i} \\ c_{2,i} \end{bmatrix} = \begin{bmatrix} J_{i-1} \\ \Psi_{proximal,i} - \Psi_{soil} \end{bmatrix} \tag{B2}$$

Inverting the system, Eq. (B2) yields:

$$\begin{cases} c_{1,i} = \frac{k_x(l_{i-1})f'_{2,i}(l_{i-1})(\Psi_{proximal,i} - \Psi_{soil}) + f_{2,i}(l_i)J_{i-1}}{k_x(l_{i-1})\left(f'_{2,i}(l_{i-1})f_{1,i}(l_i) - f'_{1,i}(l_{i-1})f_{2,i}(l_i)\right)} \\ c_{2,i} = \frac{-k_x(l_{i-1})f'_{1,i}(l_{i-1})(\Psi_{proximal,i} - \Psi_{soil}) - f_{1,i}(l_i)J_{i-1}}{k_x(l_{i-1})\left(f'_{2,i}(l_{i-1})f_1(l_i) - f'_{1,i}(l_{i-1})f_{2,i}(l_i)\right)} \end{cases} \tag{B3}$$

In homogeneous soil conditions, the proximal flow J_{i-1} may be expressed as the product of the upstream conductance

10   ($K_{rs,i-1}$ intrinsic root property) by the potential difference between the soil and the proximal xylem water potential of the root

stretch:

$$J_{i-1} = K_{rs,i-1}\left(\Psi_{soil} - \Psi_x(l_{i-1})\right) = -K_{rs,i-1}\left(c_{1,i}f_{1,i}(l_{i-1}) + c_{2,i}f_{2,i}(l_{i-1})\right) \tag{B4}$$

Substituting Eq. (B4) in Eq. (B3) for the i$^{\text{th}}$ stretch, we obtain a set of two equations with two unknowns which after solving

for $c_{1,i}$ and $c_{2,i}$ gives:

$$\begin{cases} c_{1,i} = \frac{(\Psi_{proximal,i} - \Psi_{soil})\left(-K_{rs,i-1}f_{2,i}(l_{i-1}) + f'_{2,i}(l_{i-1})k_x(l_{i-1})\right)}{K_{rs,i-1}f_{1,i}(l_{i-1})f_{2,i}(l_i) - K_{rs,i-1}f_{1,i}(l_i)f_{2,i}(l_{i-1}) - f'_{1,i}(l_{i-1})f_{2,i}(l_i)k_x(l_{i-1}) + f_{1,i}(l_i)f'_{2,i}(l_{i-1})k_x(l_{i-1})} \\ c_{2,i} = \frac{(\Psi_{proximal,i-1} - \Psi_{soil})\left(K_{rs,i-1}f_{1,i}(l_{i-1}) - f'_{1,i}(l_{i-1})k_x(l_{i-1})\right)}{K_{rs,i-1}f_{1,i}(l_{i-1})f_{2,i}(l_i) - K_{rs,i-1}f_{1,i}(l_i)f_{2,i}(l_{i-1}) - f'_{1,i}(l_{i-1})f_{2,i}(l_i)k_x(l_{i-1}) + f_{1,i}(l_i)f'_{2,i}(l_{i-1})k_x(l_{i-1})} \end{cases} \tag{B5}$$

15

It is important to mention that these coefficients only depend on the properties of the distal stretches to the stretch of interest

and on the effective conductivity that lumps the properties and their spatial variation in all distal stretches. Combining the

coefficients (B5), the definitions of the macroscopic parameters (B1) and the general solutions (5), (2) and (3), the root system

conductance and the standard uptake density after addition of i stretches become:

$$\begin{cases} K_{rs,i} = k_x(l_i)\frac{\left(-K_{rs,i-1}f_{2,i}(l_{i-1}) + f'_{2,i}(l_{i-1})k_x(l_{i-1})\right)f'_{1,i}(l_i) + \left(K_{rs,i-1}f_{1,i}(l_{i-1}) - f'_{1,i}(l_{i-1})k_x(l_{i-1})\right)f'_{2,i}(l_i)}{K_{rs,i-1}f_{1,i}(l_{i-1})f_{2,i}(l_i) - K_{rs,i-1}f_{1,i}(l_i)f_{2,i}(l_{i-1}) - f'_{1,i}(l_{i-1})f_{2,i}(l_i)k_x(l_{i-1}) + f_{1,i}(l_i)f'_{2,i}(l_{i-1})k_x(l_{i-1})} \\ SUD_i(z) = \frac{2\pi r k_r(z)}{k_x(l_i)}\frac{\left(-K_{rs,i-1}f_{2,i}(l_{i-1}) + f'_{2,i}(l_{i-1})k_x(l_{i-1})\right)f_{1,i}(z) + \left(K_{rs,i-1}f_{1,i}(l_{i-1}) - f'_{1,i}(l_{i-1})k_x(l_{i-1})\right)f_{2,i}(z)}{\left(-K_{rs,i-1}f_{2,i}(l_{i-1}) + f'_{2,i}(l_{i-1})k_x(l_{i-1})\right)f'_{1,i}(l_i) + \left(K_{rs,i-1}f_{1,i}(l_{i-1}) - f'_{1,i}(l_{i-1})k_x(l_{i-1})\right)f'_{2,i}(l_i)} \end{cases} \tag{B6}$$

20

Appendix C: Special case of a single-stretched root

If the root system consist in a single stretch, the distal boundary condition is no-flux and the proximal boundary conditions corresponds to the root collar water potential Ψ_{collar} [P]. l_1 is equivalent to l. Mathematically, the boundary conditions become:

$$
\begin{cases}
J_x(0) = 0 \\
\Psi_x(l) = \Psi_{collar}
\end{cases}
\tag{C1}
$$

5   The boundary conditions (C1) used in case of a root made of a single stretch can be rewritten as:

$$
\begin{bmatrix} -k_x(0)f_1'(0) & -k_x(0)f_2'(0) \\ f_1(l) & f_2(l) \end{bmatrix}
\begin{bmatrix} c_1^{nf} \\ c_2^{nf} \end{bmatrix}
=
\begin{bmatrix} 0 \\ \Psi_{collar} - \Psi_{soil} \end{bmatrix}
\tag{C2}
$$

As in Appendix A, the superscript nf means no-flux bottom boundary condition. It is used when the root is made of only one stretch. Inverting the matrix we obtain the constants:

$$
\begin{cases}
c_1^{nf} = \dfrac{f_2'(0)(\Psi_{collar}-\Psi_{soil})}{f_2'(0)f_1(l)-f_1'(0)f_2(l)} \\
c_2^{nf} = \dfrac{-f_1'(0)(\Psi_{collar}-\Psi_{soil})}{f_2'(0)f_1(l)-f_1'(0)f_2(l)}
\end{cases}
\tag{C3}
$$

10   The 'non-flux' coefficients (C3) are actually a particular case of the 'flux' coefficients (B5) since the latter tend to the former as $K_{rs,i-1} \to 0$ (or $J_{i-1} \to 0$).

The macroscopic parameters of the single-stretch-root branch are finally given by (using the no-flux coefficients (C3) or equivalently evaluating Eq. (B6) with $K_{rs,i-1} = 0$):

$$
\begin{cases}
K_{rs}^{nf} = k_x(l) \left(\dfrac{f_2'(0)f_1'(l)-f_1'(0)f_2'(l)}{f_2'(0)f_1(l)-f_1'(0)f_2(l)} \right) \\
SUD^{nf}(z) = \dfrac{2\pi r k_r(z)}{k_x(l)} \left(\dfrac{f_2'(0)f_1(z)-f_1'(0)f_2(0)}{f_2'(0)f_1'(l)-f_1'(0)f_2'(l)} \right)
\end{cases}
\tag{C4}
$$

Appendix D: Stretch lengths in heterogeneous root branches

Let us consider a growing root branch with an initial elongation rate $v_0\,[\mathrm{LT^{-1}}]$ and a maximal length $l_{max}\,[\mathrm{L}]$. Its actual elongation rate $v(t)\,[\mathrm{LT^{-1}}]$ is given, as in Pagès et al. (2004), at any time $t\,[\mathrm{T}]$ by:

$$v(t) = v_0 exp\left(\frac{-v_0}{l_{max}}t\right) \tag{D1}$$

5 Integrating Eq. (D1) between 0 and time t, we obtain the actual root length $l\,[\mathrm{L}]$:

$$l(t) = \int_0^t v(t')dt' = l_{max}\left[1 - exp\left(\frac{-v_0}{l_{max}}t\right)\right] \tag{D2}$$

In the case of the root made of one stretch, the root length can be easily substituted by Eq. (D2) to obtain the macroscopic parameters as a function of time instead of root length. If the root is split in distinct stretches, as we substitute l by t, we need to replace the transition positions by transition ages. An equation of the different root stretch lengths $stretch_i(t)\,[\mathrm{L}]$ is required

10 (we use the indices i to indicate the zones from the tip to the collar, see Fig. 2).

Inverting Eq. (D2), the root age $age(z,t)\,[\mathrm{T}]$ at any distance z to the root tip z and at any time t yields:

$$age(z,t) = t + \frac{l_{max}}{v_0}ln\left(\frac{z}{l_{max}} + exp\left(\frac{-v_0}{l_{max}}t\right)\right), \forall z \in [0\,l(t)] \tag{D3}$$

Equation (D3) is then used to derive the macroscopic parameters and the water flow equation solution of a single branch root as a function of age or when the root hydraulic properties are defined as a function of time instead of as a function of the

15 distance to the tip. We can also calculate the stretch lengths, $stretch_i$. When the root is older than any transition age (called hereafter $age_i\,[t]$), it is simply the length differences between two successive transition ages. When the root is younger, then either the root zone length is zero (if the young transition age is not reached yet) or growing limited by the total root length:

$$stretch_i(t) = \begin{cases} 0, t < age_i \\ l_{max}\left(1 - exp\left(\frac{-v_0}{l_{max}}(t - age_i)\right)\right), t \geq age_i \text{ and } t \leq age_{i+1} \\ l_{max}\left(exp\left(-\frac{v_0}{l_{max}}(t - age_{i+1})\right) - exp\left(-\frac{v_0}{l_{max}}(t - age_i)\right)\right), t > age_{i+1} \end{cases} \tag{D4}$$

Author contributions. F. Meunier solved the water flow equation with the help of V. Couvreur and developed the model used in the simulations. J. Vanderborght, V. Couvreur M. Javaux and X. Draye suggested simulations to illustrate the model and help in the model conception. F. Meunier prepared the manuscript with contributions from all co-authors.

Competing interests. The authors declare that they have no conflict of interest.